Smart Processing Technology, Vol. 1 (2006)
High Temperature Society of Japan

ELECTRON-HOLES BEHAVIROS IN TiO_2-Fe_3O_4 COATING DEPOSITED BY PLASMA SPRAYING FOR ENVIRONMENTAL APPLICATION

Fuxing Ye, Akira Ohmori, Takuya Tsumura, and Kazuhiro Nakata

Joining and Welding Research Institute, Osaka University,
11-1, Mihogaoka, Ibaraki, Osaka, 567-0047, Japan

Photocatalyst has been attracted great attention in recent years to purify the polluted environment and to avoid further pollution. To develop more effective photocatalyst with cost effective plasma spraying, TiO_2 and composite TiO_2-Fe_3O_4 coatings were deposited using agglomerated anatase nano-TiO_2 and composite TiO_2-Fe_3O_4 powders, respectively. The electron-holes behaviors in composite TiO_2-Fe_3O_4 coating comparing with TiO_2 coating were investigated through a three-electrode cell and photocatalytic evaluation apparatuses. The short-circuit current of TiO_2-Fe_3O_4 coating was 15 times lower than that of TiO_2 coating under 30 mW/cm^2 xenon light illumination. In the heating, impacting, flattening and rapid solidification processes of the feedstock powder in plasma spraying, nano-TiO_2 semiconductor particle reacted with Fe_3O_4 and/or Fe_2O_3 and concurrently produced p-type $FeTiO_3$, which substantially improved the photocatalytic performance of the TiO_2 coating for the formation of p-$FeTiO_3$/n-TiO_2 junction which resulted in spatially separation of photo-generated electrons and holes and then greatly improved their efficiency for the photocatalysis.

Keywords: plasma spraying, photocatalyst, TiO_2, $FeTiO_3$.

1. INTRODUCTION

Photocatalysis by semiconductor is the result of the interaction of electrons and holes generated in an activated solid with the surrounding medium (Alfano, et al., 2000). The activation behavior has similarity to that of *Si* solar cell. The fundamental principle of photocatalysis is the same as that of photo-electrochemistry, which originates from electron-hole pair generation and efficient separation. As presented in our previous article (Ye and Ohmori, 2002), multiple-band-gap photocatalytic reaction cell formed in composite TiO_2-Fe_3O_4 coating. Moreover, $FeTiO_3$ is a kind of p-type semiconductor (Ishikawa and Sawada, 1956) and TiO_2 is a kind of n-type semiconductor, thus solid p-n junction formation between p-$FeTiO_3$ and n-TiO_2 in the sprayed coating is possible in thermal spraying process.

The formation of a plasma sprayed deposit is formed by a stream of molten droplets impacting on the substrate followed by flattening, rapid solidifying and cooling process. The individual molten (or half-molten) droplets spread to thin splat/lamellae, the stacking of which constitutes the deposit (Li and Ohmori, 2002). Furthermore, it is easy to deposit composite coatings by plasma spraying technique if the feedstock powders are composite materials. The composite substances may react with each other and then produce new compounds in the heating process; and the interface between two kinds of compounds is very large because the droplets spread to very thin lamellae (micron order). Therefore, the formation of microelectrochemical cell between two individual splats is reasonable. One splat is photo-anode and another is regarded as photo-cathode.

With respect to upper supposition, examinations on the photoelectrochemical characteristics of plasma sprayed TiO_2 and TiO_2-Fe_3O_4 electrodes were motivated to investigate their electron-holes behaviors. Moreover, TiO_2-Fe_3O_4 splat was formed and its element distributions were analyzed.

2. MATERIALS AND EXPERIMENTAL PROCEDURE

2.1 Materials

The feedstock powders were agglomerated TiO_2 powder and TiO_2-Fe_3O_4 composite powder. The substrate for electrode or coating preparation was stainless steel (JIS SUS304). However, to analyze the *Fe* element distribution in the splat, the substrate for splat formation was copper, otherwise the *Fe* element from steel substrate will disturb the EDAX analysis.

2.2 Plasma spraying equipment

Thermal spray equipment was a commercial plasma spray system with a SG-100 plasma spray torch. Argon was used as a primary plasma gas and helium was used as the secondary gas. The thermal spraying parameters are given in Table1.

Table 1: Plasma spraying parameters.

Argon gas pressure (MPa) /flow (slpm)	0.42/58
Helium gas pressure (MPa) /flow (slpm)	0.21/9
Arc current (A)	600
Arc voltage (V)	28
Spraying distance (mm)	70

2.3. Characterization of sprayed coatings, splat and electrodes

Microstructure and phase characterization of sprayed coatings and splat were performed by electron probe surface roughness analyzer, energy dispersive analysis of x-ray (ERA-8800FE, Elionix Co. Ltd., Japan) and x-ray diffraction (JDX3530, JEOL, Japan).

The photocatalytic activity of the sprayed coatings was evaluated through the degradation of acetaldehyde under 1 mW/cm^2 ultraviolet light irradiation. The photocatalytic activity was defined as the reciprocal of τ value. The smaller the value of τ the better of photocatalytic activity of the coating. The details were described elsewhere(Ye and Ohmori, 2002).

The photoelectrochemical characteristics of plasma sprayed coatings were studied through a three-electrode cell system under xenon light irradiation. The photocurrent against potential at each sprayed electrode (10×10 mm) was measured using a scanning potentiostat. The sweep speed of the potential was 2mV/s in every experiment. A 500W xenon lamp was used as light source and the light intensity was measured by a UV radiometer (UVR-2, TOPCON, Tokyo, Japan) with UD-40.

3. RESULTS AND DISSCUSSION

3.1 Structure and compositions of TiO_2 and TiO_2-Fe_3O_4 coatings

The surface morphologies of TiO_2 and TiO_2-Fe_3O_4 coatings prepared by plasma spraying technique under arc current of 600 A are shown in **Fig.1**. In the figures, "U", "P" and "M" denote un-melted zone, partially melted zone and melted zone, respectively. In the sprayed coatings, TiO_2-Fe_3O_4 powders were more melted than TiO_2 powders. This phenomenon was similar to that of the same kinds of coatings prepared at relative low arc current of 400 A and 500 A (Ye and Ohmori, 2002).

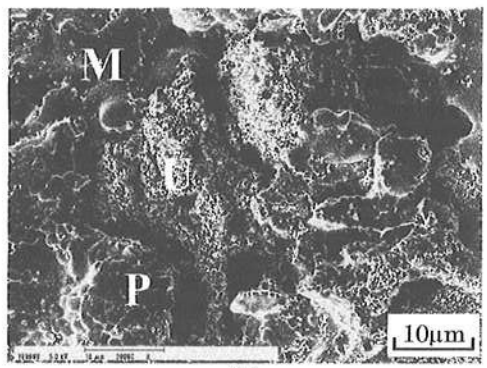

(a)

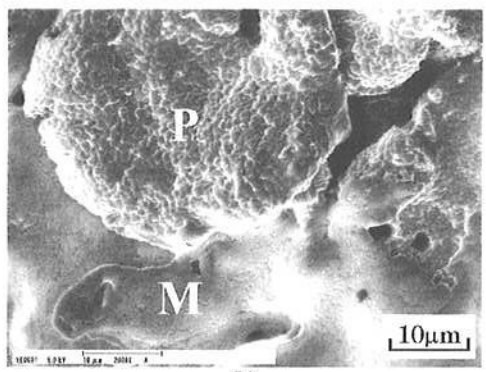

(b)

Fig.1. Surface morphologies of TiO_2 (a) and TiO_2-Fe_3O_4 (b) coatings sprayed under the current of 600 A. (Notes: "U", "P" and "M" denote un-melted zone, partially melted zone and melted zone, respectively.)

According to the x-ray diffraction pattern of plasma sprayed TiO_2-Fe_3O_4 coating, it consisted of rutile

TiO_2, anatase TiO_2 and $FeTiO_3$. One part of Fe_3O_4 reacted with O_2 and produced Fe_2O_3, and TiO_2 reacted with Fe_3O_4 or Fe_2O_3 and formed $FeTiO_3$.

3.2 Characterization results of TiO_2-Fe_3O_4 splat

Fig. 2 shows the SEM view of TiO_2-Fe_3O_4 splat, and Ti, Fe elements distribution of *line A* illustrated in it. The splat was very thin and the Ti and Fe elements distributed uniformly. The Fe/(Fe+Ti) ratio in the TiO_2-Fe_3O_4 splat was approximates to 0.12, which is in good agreement with the amount of the feedstock powder.

3.3 Photocatalytic activity of TiO_2 and TiO_2-Fe_3O_4 coatings

The photocatalytic degradation efficiency of TiO_2-Fe_3O_4 coating was approximately two times higher than that of TiO_2 coating. The good photocatalytic activity of TiO_2-Fe_3O_4 coating partly resulted from the good light absorbance and the good electron-hole separation character of $FeTiO_3$ while TiO_2 coexists, which was explained by the two-steps photoexcitation model (Ye and Ohmori, 2002). Because of the existance of the two-steps photoexcitation phenomenon in TiO_2-Fe_3O_4 coating, the light absorption edge shifts to longer wavelength and the separation of excited electron-holes is improved. Another reason for the good photocatalytic activity of TiO_2-Fe_3O_4 coating is given in ***Section 3.5***.

3.4 Photoelectrochemical characteristics of TiO_2 and TiO_2-Fe_3O_4 electrodes

Fig. 3 illustrates the photocurrent-potential curves with and without xenon light irradiation of the TiO_2 electrode prepared under arc current of 600 A. The photocurrent increased obviously from the applied potential of −0.6 V to −0.3 V, and then increased slightly till 0.4 V, and finally broke. The photo-response characteristic of the sprayed electrode was comparable to that of single crystal TiO_2 (Wang, 1979), but the breakdown voltage was approximate to 0.5 V (vs. SCE). The short-circuit current (Jsc) of TiO_2 electrode was 1.05 mA/cm^2 under 30 mW/cm^2 light illumination from xenon lamp. Under the dark condition, the short-circuit current (Jsc) of TiO_2 electrode was approximate to zero.

Fig. 4 illustrates the photocurrent-potential curves with and without xenon light irradiation of the TiO_2-Fe_3O_4 electrode prepared under arc current of 600 A. The photocurrent increased slightly from the applied potential of −0.6 V to 0.4 V, and then broke over 0.5 V. The short-circuit current (Jsc) of TiO_2-Fe_3O_4 electrode was 0.07 mA/cm^2, which was notably lower than that of TiO_2 electrode under 30 mW/cm^2 xenon light illumination. However, the bubbles (came from water photolysis) formation speed from TiO_2-Fe_3O_4 electrode was about three times higher than that from the latter. Under the dark condition, the short-circuit current (Jsc) of TiO_2-Fe_3O_4 electrode was the same as that of TiO_2 electrode.

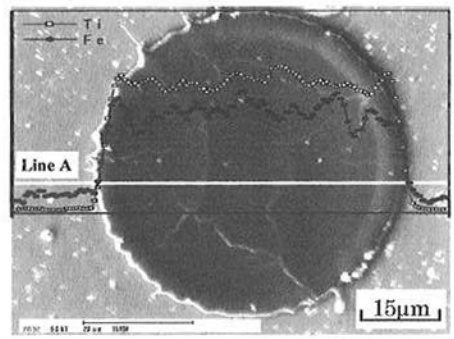

Fig.2. SEM view of TiO_2-Fe_3O_4 splat, and Ti, Fe elements distribution of *line A* illustrated in SEM view.

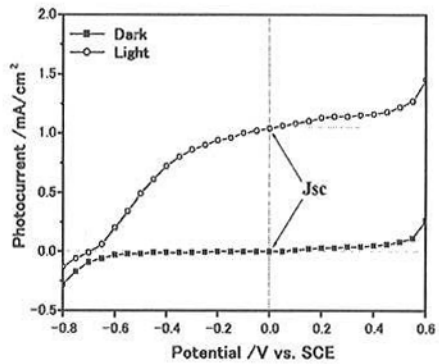

Fig.3. Photocurrent-potential curves with and without light irradiation of the TiO_2 electrode prepared under arc current of 600 A.

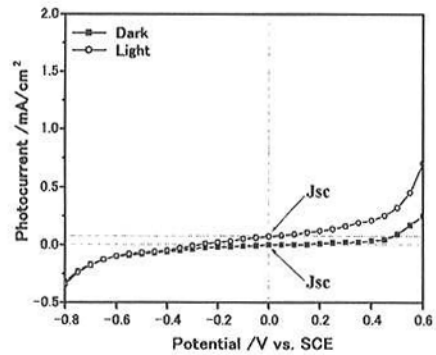

Fig.4. Photocurrent-potential curves with and without light irradiation of the TiO_2-Fe_3O_4 electrode prepared under arc current of 600 A.

3.5 P-N junction formation model

According to the x-ray diffraction pattern, the n-type TiO_2 semiconductor particle reacted with Fe_2O_3 or Fe_3O_4 particle and concurrently produced p-type $FeTiO_3$ in the TiO_2-Fe_3O_4 coating, thus solid p-n junction formation between p-type $FeTiO_3$ and n-type TiO_2 in the sprayed TiO_2-Fe_3O_4 coating was possible in thermal spraying processes. The bubbles (came from water photolysis) formation speed from TiO_2-Fe_3O_4 electrode was higher than that from TiO_2 electrode. Furthermore, H_2 and O_2 generation coincided on TiO_2-Fe_3O_4 electrode. Moreover, the short-circuit current (Jsc) of TiO_2-Fe_3O_4 electrode was notably lower. These facts implied that the $FeTiO_3$/TiO_2 island acted as microphoto-electrolysis cell in a short circuit configuration in TiO_2-Fe_3O_4 coating. Therefore, the existence of solid p-n junction between p-type $FeTiO_3$ and n-type TiO_2 was confirmed.

According to the above-mentioned results and the special particle flattening phenomenon in plasma spraying processes, a p-n junction formation model in plasma sprayed TiO_2-Fe_3O_4 coating is illustrated in **Fig.5a**. In fact, an agglomerated TiO_2-Fe_3O_4 powder contains many micro TiO_2 particles with average diameter of 200 nm, therefore, it is reasonable that one small splat flattened from primary TiO_2 particle may generate a micro p-n junction with $FeTiO_3$, and then it is inferred that a TiO_2-Fe_3O_4 splat shown in Fig.2 comprised a lot of micro p-n junctions. **Fig.5b** shows the schematic diagram of electron-hole separation process in a p-n junction. The micro-TiO_2 and $FeTiO_3$ constituted innumerable micro-cell.

For the formation of micro p-n junction, which may spatially separate the photo generated electrons and holes as like Si solar cell, the photocatalytic activity of TiO_2-Fe_3O_4 coating was improved significantly as given in ***Section 3.3***. As a result, plasma-sprayed TiO_2-Fe_3O_4 coatings are promising candidates for the applications to photocatalyst.

4. CONCLUSIONS

The electron-hole behaviors in composite TiO_2-Fe_3O_4 coating comparing with TiO_2 coating were examined in this study. The photo-response of the sprayed TiO_2 electrode was comparable to that of single crystal TiO_2, but the breakdown voltage was approximately 0.5 V (vs. SCE). The short-circuit current of TiO_2 was 1.05 mA/cm^2, which was 15 times higher than that of TiO_2-Fe_3O_4 electrode under 30 mW/cm^2 light illumination from xenon lamp. $FeTiO_3$ compound obviously improved the photocatalytic activity of the TiO_2 coating for the formation of p-n junction between p-$FeTiO_3$ and n-TiO_2, which may spatially separate the photo-generated electrons and holes and then greatly improved the photocatalytic efficiency of composite TiO_2-Fe_3O_4 coating.

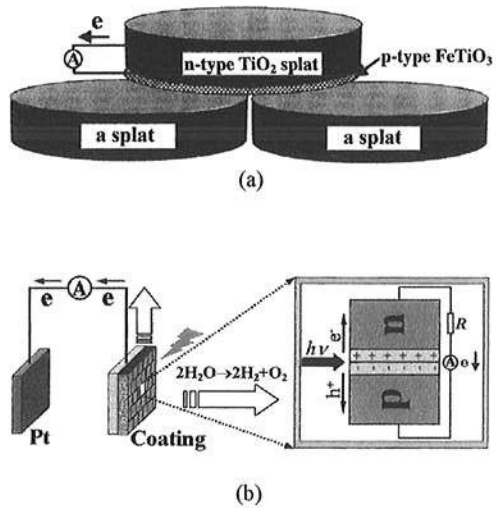

Fig.5. A proposed p-n junction formation model (a) and schematic diagram of electron-hole separation process (b) in the TiO_2-Fe_3O_4 coating.

REFERENCES

Alfano M., D. Bahnemann, A. E. Cassano, R. Dillert, and R. Goslich (2000). Photocatalysis in water environments using artificial and solar light. *Catalysis Today*, **58**, 199-230.

Ishikawa Y. and S. Sawada (1956). The study on substances having the ilmenite structure, physical properties of synthesized $FeTiO_3$ and $NiTiO_3$ ceramics. *Journal of Physical Society of Japan*, **11**, 496-501.

Li C. J. and A. Ohmori (2002). Relationships between the microstructure and properties of thermally sprayed deposits. *Journal of Thermal Spray Technology*, **11**, 365-374.

Ye F. X. and A. Ohmori (2002). The photocatalytic activity and photo-absorption of plasma sprayed TiO_2-Fe_3O_4 binary oxide coatings. *Surface and Coatings Technology*, **160**, 62-67.